Numerical Investigation of Non-Newtonian Laminar Flow in Curved Tube with Insert

A. Kadyyrov[1]
[1] Research center for power engineering problems Federal government budgetary institution of science Kazan scientific center Russian Academy of Sciences,
*Corresponding author: Russia, Kazan, 420111, Lobachevsky St 2/31, In box 190, aidarik@rambler.ru

Abstract: Non-Newtonian laminar flows in curved circular tubes with inserts are investigated by computer simulations. 0.65% solution of NaCMC is considered. Three-dimensional incompressible Navier-Stokes equations are solved using COMSOL Multiphysics. Placements of inserts inside the curved tubes and their effects on the hydrodynamics of the flow are studied. Computations are carried out with various values of Reynolds number ranging from 10 to 1000.

Keywords: Non-Newtonian, curved, tube, insert.

1. Introduction and Governing Equations.

Heat transfer processes are known to depend on hydrodynamic fields. Therefore, the purpose of this research is to study the hydrodynamic fields in curved channels. We consider a steady flow of Non-Newtonian viscous liquids in a curved tube. The mathematical model is developed taking into account a negligibly small gravity force.

The steady three-dimensional Navier-Stokes equations are used as the governing equations:

$$\rho(\mathbf{u}\cdot\nabla)\mathbf{u} = \nabla\cdot\left(-\mathrm{pI}+\mu\left(\nabla\mathbf{u}+(\nabla\mathbf{u})^{\mathrm{T}}\right)\right) \text{ in } \Omega \qquad (1)$$

$$\nabla\cdot\mathbf{u} = 0 \text{ in } \Omega \qquad (2)$$

where $\mathbf{u}=(u1,u2,u3)$ is the fluid velocity, p is pressure, μ and ρ are viscosity and density of the fluid respectively. The solution domain Ω (Fig. 1) consists of three parts. The first part is a part of a straight tube of 0.015m long, L1=0.01 m, L2=0.005 m. The second part is a curved region with rotation angle α=90º and radius of the curvature R=0.075m. The third part is a part of the straight tube following the curved part. Boundary conditions: in the inlet region of the channel velocity field is fully developed, in the outlet region of the channel normal stress is given (the total stress on the boundary is set equal to a stress vector of magnitude, $f_0 = 0$ oriented in the opposite normal direction). The no-slip condition is forced on the channel walls.

We consider two geometric objects. There is a twisted tape insert in the curved part between B and F in Elbow #1 (Fig. 1). Elbow #2 has a twisted tape insert in the straight part of the tube between A and B. The tape is twisted until it reaches an angle of 90 degrees and turns right in both cases.

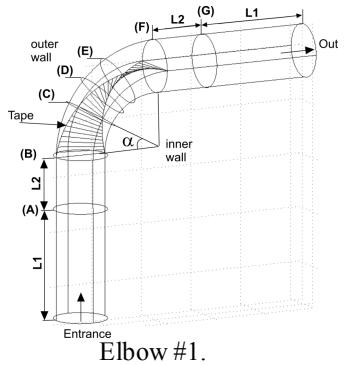

Elbow #1.

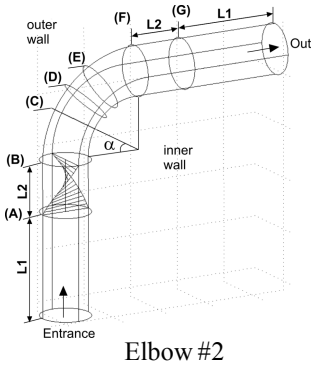

Elbow #2

Figure 1. Geometric objects, (A), (B),…, (G) – cross-sections, where (C) – 30º cross-section, (D) – 45º cross-section, (E) – 60º cross-section.

To describe the viscosity behavior we used the Kutateladze model [1]. It is based on the structural theory of viscosity and its parameters have physical meaning. The rheological properties of Carboxymethyl cellulose (0.65%

NaCMC) depend on strain and do not depend on their previous history.

$$\varphi_* = \exp(-\tau_*), \quad (3)$$

where $\varphi_* = (\varphi_\infty - \Phi)/(\varphi_\infty - \varphi_0)$, $\tau_* = \theta(\tau - \tau_1)/(\varphi_\infty - \varphi_0)$, $\tau = \varphi_1(I_2)\sqrt{I_2/2}$; $\Phi = 1/\varphi_1(I_2)$ is fluidity; φ_0, φ_∞ - fluidity when $\tau \to 0$, $\tau \to \infty$ respectively; θ is a measure of the structural stability of the fluid; τ_1 is yield stress; $I_2 = 4\mathrm{tr}\mathbf{D}^2$ is the second invariant of the strain rate tensor. In addition, $\theta = 0$ corresponds to a Newtonian fluid, $\theta < 0$ corresponds to a dilatant fluid, $\theta > 0$ corresponds to a pseudo-plastic fluid.

The three-dimensional incompressible Navier-Stokes equations are solved using COMSOL Multiphysics. To solve linear system equations we used "Direct (PARDISO)". In our computations we examined Sodium Carboxymethyl cellulose (0.65% NaCMC) (Fig. 2). This fluid is one of the widely used as a non-Newtonian fluid.

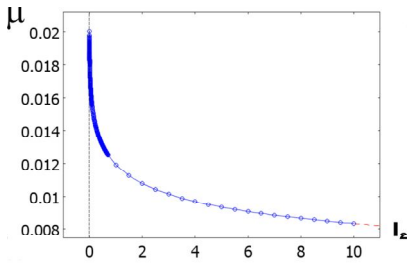

Figure 2. Dependence of dynamic viscosity (Pa·s) on the second invariant of the strain rate tensor (s^{-2}) for Sodium Carboxymethyl cellulose (0.65% NaCMC), T=303K.

An actual engineering problem is used to validate the code of COMSOL Multiphysics and partitioning mesh. The experimental results of Muguercia et al. [2] are compared with the simulated data obtained numerically. In these laboratory tests, a 180° U-tube, with the straight tube preceding its inlet ensures that flow is fully developed. The U-tube has the radius of curvature R = 6.35 cm and the radius of the cross section a=1.1 cm. Fully developed flow condition is simulated with Reynolds numbers of 1000, which correspond to Dean numbers of 416. The fluid being tested (58-60% benzyl alcohol in 95% ethyl alcohol) has a density of 0.931 g/cm3 and an absolute viscosity of about 0.03 g/cm/sec. Mesh generation starts with a coarse initial mesh. The volume of the mesh is then improved by refining the initial mesh step by step. The refinement process is controlled by calculation of the integral value of velocity at the cross-section (D). The refinement process is finished when the relative error becomes less than 0.001. In this case the mesh consists of 241408 elements. The computations are performed on the computer Intel® CoreTM i7 950 with 24Gb RAM. A comparison is presented in Fig. 3.

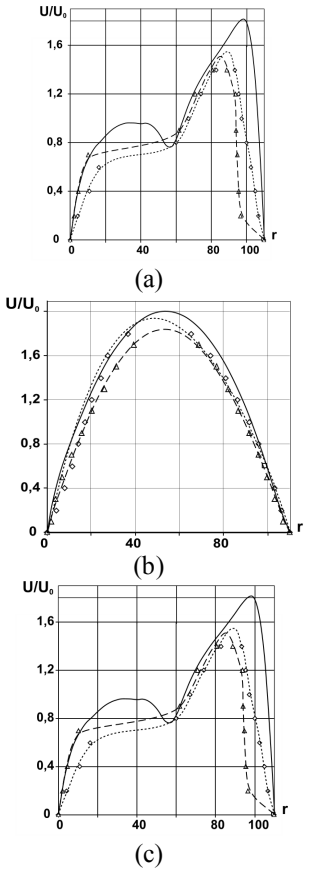

Figure 3. The distribution of relative velocity at the cross section; a) at the entrance; b) at the 90° cross section; c) at the 180° cross-section; continuous line - numerical result; diamonds - numerical result of Guan, Xiaofeng [3]; triangles - experimental result of Muguercia [2].

2. Numerical Results

Numerical computations are carried out with the help of COMSOL Multiphysics using

Lagrange P_2P_1 elements over a trihedral mesh. The computational mesh consists of 220342 and 220322 elements for elbow #1 and elbow #2 respectively. The twisted tapes are designed and then imported from MatLab. The calculations are performed for ρ = 1012 kg/cm3 and the temperature 303K. On the Fig. 4 are presented the velocity field.

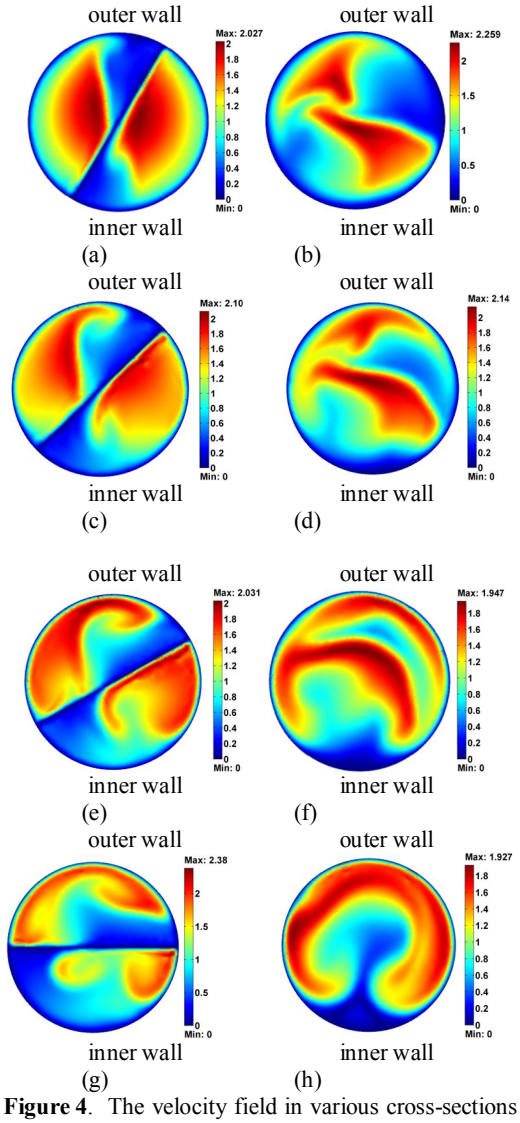

Figure 4. The velocity field in various cross-sections of the curved channel with inserts; (a) at cross-section C, Elbow #1; (b) at cross-section C, Elbow #2; (c) at cross-section D, Elbow #1; (d) at cross-section D, Elbow #2; (e) at cross-section E, Elbow #1; (f) at cross-section E, Elbow #2; (g) at cross-section F, Elbow #1; (h) at cross-section F, Elbow #2; Re=1039.

In the curved channel the fluid particles with different speeds are subjected to different effects of centrifugal forces. Due to these forces maximum speed tends to the outer wall of the curved tube. Numerical results show that due to the twisted tape inserted into the curved part of the channel additional inertial forces appear. Therefore, the fluid flow moves quicker to the outer walls of the channel passing throughout the curved part (Elbow # 1). If there is the insert in front of the curved part additional inertial forces contribute to the fact that the region with the maximum speed is achieved in the central part of the curved channel from section C to E (Elbow # 1).

The region of maximum pressure is known to be located on the outer wall of the curved tube (Fig. 5 c, f, i) and remains virtually unchanged throughout its length.

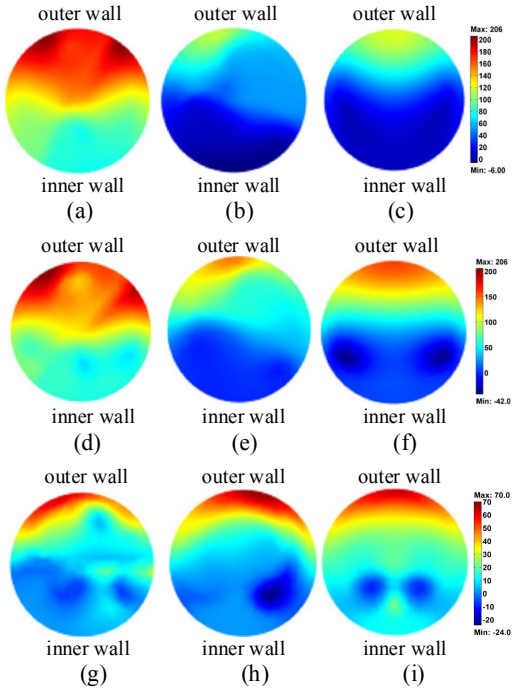

Figure 5. Pressure distribution in various cross-sections of the curved channel with inserts; (a) at cross-section C, Elbow #1; (b) at cross-section C, Elbow #2; (c) at cross-section C, curved channel without inserts [4]; (d) at cross-section D, Elbow #1; (e) at cross-section D, Elbow #2; (f) at cross-section D, curved channel without inserts [4]; (g) at cross-section F, Elbow #1; (h) at cross-section F, Elbow #2; (i) at cross-section F, the curved channel without inserts [4]. Re=1039.

Moreover, the maximum value itself varies and reaches its maximum in section D. The presence of inserts inside the curved tube alters the pressure distribution and its maximum value. In Elbow # 1 the region of maximum pressure is somewhat moved from the outer wall, but the maximum value is much higher than the values in tubes without inserts. In Elbow #2 though the pressure distribution is asymmetrical, in general it follows the distribution in the tube without inserts. It should be emphasized that maximum pressure in this case is lower than corresponding values in tubes without inserts (for example, in section D, a decrease of the maximum pressure on the outer wall reaches 8%).

In Fig.6 the pressure distribution on the wall of the channel is shown. Two areas with high pressure in elbow #1 can be clearly seen. Using this twisted tape in the curved channel (as elbow #2) makes it possible to reduce pressure and decrease the area with high pressure on the outer wall.

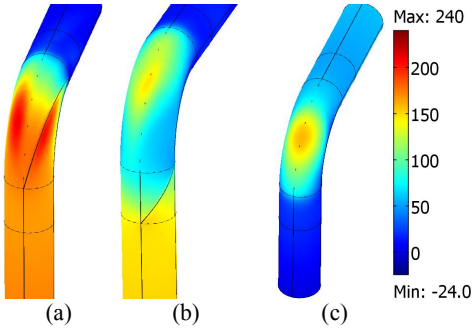

Figure 6. Pressure distribution on the walls; (a) Elbow #1; (b) Elbow #2; (c) the curved tube without insert; Re=1039.

The relation between presence of the insert in the curved tube and the hydraulic resistance coefficient is shown in Fig.7. Postprocessing of the obtained results showed that, due to the insert in the curved tube, as considered in Fig. 1, the hydraulic resistance coefficient increases. For example, ξ_G for elbow #2 is 220% more than ξ_{BF} for the curved tube without insert for Re=1039. Using the twisted tape directly before the curved region is helpful for steeply curved channels because the area of high velocity moves towards the center of the curved channel.

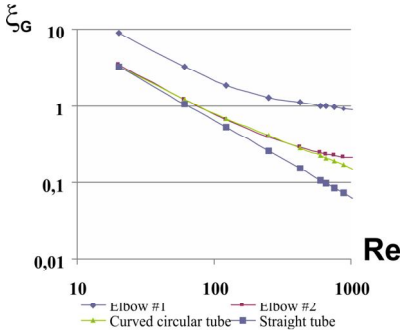

Figure 7 (a)

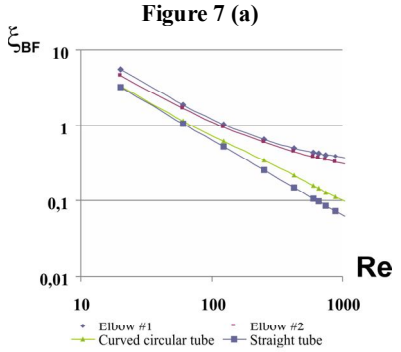

Figure 7 (b)

Figure 7. Hydraulic resistance coefficient as a function of Reynolds number; ξ_G – hydraulic resistance coefficient between cross-sections (Entrance) and (G); ξ_{BF} – hydraulic resistance coefficient between cross-sections (B) and (F) (Fig. 1).

3. Conclusions

Laminar flow in the curved channels with different placements of inserts is considered. For elbow #2 the most part of high velocity area is located in the center of the channel throughout its length. The twisted tape before the curved channel considered for elbow#2 reduces the pressure on the outer wall and consequently reduces the force on the pipe wall and increases its longevity. The calculated hydrodynamic parameters can be further used to calculate heat and mass transfer.

4. References

1. Kutateladze S.S., Popov V.I., Khabakhpasheva E.M. Hydrodynamics of fluids of variable viscosity, *Journal of Applied Mechanics and Technical Physics*. **No 1**, pp. 45-49 (1965)

2. Muguercia, I., Cazanas, B., Ebadian, M.A. Measurements of the Secondary Velocity Vector in a 180 U-Tube Using a 2-D LDA System with a Refractive Index Matching Technique, *SPIE*, **No. 2052**, pp. 103–110 (1993)
3. Guan, Xiaofeng and Martonen, Ted B., Simulations of Flow in Curved Tubes, *Aerosol Science and Technology*, **26: 6**. pp. 485—504 (1997)
4. Kadyirov A.I., Vachagina E.K. The investigation of non-Newtonian laminar flows in a curved channel, *Thermophysics and Aeromechanics*, **V. 19**, № 3, pp. 279-289 (2012)

5. Acknowledgements

The reported study was partially supported by RFBR, research project No. 12-08-09386-mob_z.